International Science and Technology Journal
المجلة الدولية للعلوم والتقنية
Volume32العدد
Part 2 المجلد
July 2023 يوليو
المجلة الدولية للعلوم والتقنية
ISTJ

تم استلام الورقة بتاريخ: 26 / 6 /2023م وتم نشرها على الموقع بتاريخ: 30 / 7 /2023م

Influence of Sintering Temperature on β (Mg17Al12) Phase of AZ31Alloy Produced by Gas Atomization Method

Kamal Mohamed Akra[1],Ahmed Ashur Abdelhafid[2], Mustafa Boz[3]

[1]University of Zawia, Faculty of Natural Resources Engineering, Zawia, Libya
[2]University of Tripoli, Faculty of Engineering, Mechanical Engineering Department, Tripoli, Libya

[3]Karabuk University, Faculty of Technology, Department of Manufacturing Engineering, Karabuk, Turkey

k.akra@zu.edu.ly,a.abdelhafid@uot.edu.ly, mboz@karabuk.edu.tr

Abstract

In this study, the effect of sintering temperatures were investigated experimentally on the (β) (Mg17Al12) phase formed at the grain boundaries of the AZ31 alloy produced via the gas atomization method. This was achieved through tests carried out on pressed powder under pressure of about 600 MPa and different sintering temperatures of about 500, 550 and 600 °C. The SEM images were obtained and examined. The images showed that the phase β (Mg17Al12) which was formed at the grain boundaries started to spread to the surface with the increase of the temperature. In addition, the effect of temperature was evident through the occurrence of shrinkage of the grains. This can be practically explained by the increase in temperature and the increase of plastic deformation in powders. After a certain value, the powders were resistant to deformation and consequently disintegration occurred. The effect of temperature was not only spread on the grain boundaries but also throughout the whole structure.

Key words: Gas atomization, AZ31 alloy powder, sintering temperature.

International Science and Technology Journal
المجلة الدولية للعلوم والتقنية
Volume32العدد
Part 2 المجلد
July 2023 يوليو
المجلة الدولية للعلوم والتقنية
ISTJ

تم استلام الورقة بتاريخ: 26 / 6 /2023م وتم نشرها على الموقع بتاريخ: 30 / 7 /2023م

تأثير درجة حرارة التلبيد على طور (Mg17Al12) βلسبيكة ماغنيسيوم Az31 المنتجة بطريقة تذرية الغاز

كمال محمد عكرة[1]، أحمد عاشور عبد الحفيظ [2]، مصطفى بوز[3]

[1]كلية الموارد الطبيعية, جامعة الزاوية, ليبيا

[2]كلية الهندسة , جامعة طرابلس, ليبيا

[3] كلية التقنية قسم التصنيع الهندسي, جامعة كارابوك, تركيا

k.akra@zu.edu.ly,a.abdelhafid@uot.edu.ly, mboz@karabuk.edu.tr

الملخص

في هذه الدراسة، تم دراسة تأثير درجات حرارة التلبيد بشكل تجريبي على الطور(β Mg17Al12) المتكون عند حدود حبيبات سبيكة AZ31 الناتج عن طريق طريقة الانحلال الغازي. للقيام بذلك ، يتم إجراء الاختبارات عند ضغط مسحوق بضغط 600 ميجا باسكال بدرجة حرارة تلبيد 500 و 550 و 600 درجة مئوية . عند فحص صور SEM ، يُلاحظ أن المرحلة (Mg17Al12) β المتكونة عند حدود حبيبات تبدأ في الانتشار إلى السطح مع ارتفاع درجة الحرارة. يمكن تفسير ذلك من خلال زيادة درجة الحرارة وزيادة تشوه في المساحيق. بعد قيمة معينة تكون المساحيق مقاومة للتشوه ويحدث التفكك ،بينما صور المجهر الضوئي لمساحيق AZ31 Mgالمضغوطة عند ضغط 600 ميجا باسكال ، 600 ، 550 و 500 درجة مئوية ، من الواضح أن طور β (Mg17Al12) المتكون عند حدود حبيبات يزداد مع زيادة درجة الحرارة. بالإضافة إلى ذلك ، يمكن رؤية المرحلة (Mg17Al12) β بوضوح على الصور المعطاة المحاطة بحبيبات ، لوحظ ايضا أن المرحلة (Mg17Al12) β مع تأثير درجة الحرارة لا تنتشر فقط على حدود الحبيبات ولكن أيضًا في جميع أنحاء الهيكل. استنتجت هذه العلاقة من رسالتي في الدكتوراه التي التي كانت قي معامل جامعات (كارابوك، بارتن و كستامونو (

تم استلام الورقة بتاريخ: 26 / 6 /2023م وتم نشرها على الموقع بتاريخ: 30 / 7 /2023م

الكلمات المفتاح: تذرية الغاز، سبيكة ماغنيسيوم Az31، درجة حرارة التلبيد

1. Introduction

Magnesium is known as the lightest engineering metal having a density of 1.74 g/cm^3, that is 35% less than aluminum and 75% less compared to primary metals used today [1,2,3]. In comparison, magnesium has a remarkable hardness and brings many benefits such as better specific strength and increased absorption capacity [2,4]. The AZ31 series alloys are one of the most common magnesium alloys thanks to their lower cost, better resistance to corrosion as well as mechanical strength obtained through adding aluminum, zinc and manganese [5,6]. In this family of alloys, the AZ31 alloy has additional structural strength since it precipitates from the magnesium matrix and forms dual precipitates with aluminum and manganese [7,8]. Furthermore, as it adds to the strength of these materials with fine microstructures, producing them with low formability such as that of magnesium's and their alloys with powder metallurgy today has turned into a necessity in the industry. For this reason, powder metallurgy has been proved to be an option in manufacturing methods like casting, hot and cold pressing, and machining. Whereas coarse-structured microstructures can be formed via casting, powder metallurgy is regarded as a useful method so as to come up with finer microstructures [9,10]. Making composites with the help of the powder metallurgy method, characteristics like increased surface wear resistance, surface friction and surface tensions can be achieved at high temperature [11,12]. Powder production technique using this method can be carried out in four different ways: mechanical, chemical, electrolysis, and atomization. Among the other methods, gas atomization is the most common for the purpose of obtaining fine and spherical powders. The primary reason for demand behind spherical powder material is that powder-powder contact in pressing and sintering stages has to be both homogeneous and multi-directional [1,13,14]. In this respect,

تم استلام الورقة بتاريخ: 26 / 6 /2023م وتم نشرها على الموقع بتاريخ: 30 / 7 /2023م

atomization can be described as the degradation and solidification of molten metal into tiny droplets using either water, air and gas pressures or mechanical pressure. In return, the atomization process has 4 different forms: water atomization, gas atomization, centrifugal atomization, and vacuum atomization. Producing over 60% of the metal and nonmetallic powders with gas atomization makes has made this specific method an advantageous one over the other forms. Gases including air, nitrogen, argon and helium can be applied as pressurized fluid so as to decompose the liquid metal bundle in gas atomization [15]. In other words, one can produce any form of metal and alloy powder which can be melted using the gas atomization method. In doing so, there are major factors at play, mainly the type of gas, its pressure, nozzle diameter and melting temperature. As the gas pressure is added, the temperature and viscosity of the molten material tend to drop, thereby allowing the formation of smaller powders [16,17].

2. Sintering

Sintering is a kind of heating process, which enables the bonded powdered metal parts to connect to each other and provides significant strength increase and improvement of the properties. For sintering to be effective, the most important factor is the contact of the powders with each other. In this context, sintering is applied to pressed or molded powders [18]. Sintering is the heat treatment of the pressed parts in order to obtain the desired properties in a controlled atmosphere and at high temperature. In the case of sintering temperature; 70% to 80% of the melting temperatures of the metals are taken, while the sintering temperature in some refractory materials reaches up to 90% of the melting temperature. The sintering temperature can be mixed with more than one material and the pressed parts can be above the melting temperature of some components. In such cases, materials with a low melting temperature melt and fill the gaps between powders with high melting temperatures [19,20].

The sintering process usually occurs in 3 stages (Figure 1). These;

1. Burning or cleaning zone

تم استلام الورقة بتاريخ: 26 / 6 /2023م وتم نشرها على الموقع بتاريخ: 30 / 7 /2023م

2. High temperature zone
3. Cooling zone

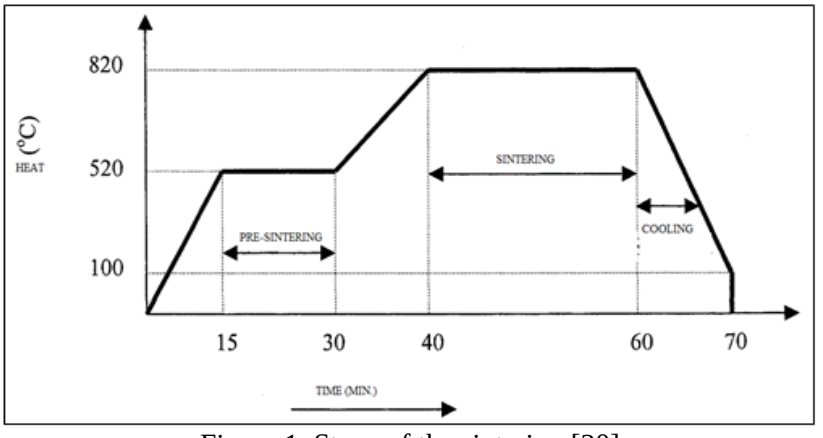

Figure 1. Stage of the sintering [20]

The first combustion and cleaning zone is the area where oil and binders are removed by air burning. Cleaning of lubricants and binders in the material occurs at low heating speeds. At high heating speeds; the binder and air, which usually burn in the pores, cause internal fragmentation by causing internal pressure. Bonds begin to form between the particles in the high temperature zone. This process occurs by solid state diffusion. The formation of intermetallic phases and solid solutions occurs by means of solid state diffusion. At the high temperature, a bond is formed between the contacting parts and this bond is strengthened by the mutual transfer of atoms. The waiting time in this region varies according to the desired density and characteristics. Waiting time is usually 10 min. between several hours. Oxidation is prevented as the cooling zone is made under atmospheric control. Since fine powder particles do not provide full contact before sintering and contain residual porosity, atmosphere control must be present in these 3 steps [16]. Another measure of sintering is determined as the ratio of neck diameter to sphere diameter. (X/D) and the neck diameter as determined by Figure 2. The region indicated by P in the figure is

تم استلام الورقة بتاريخ: 26 / 6 /2023م وتم نشرها على الموقع بتاريخ: 30 / 7 /2023م

called the radius of the neck circular profile. In addition to the actual neck growth, a sintered mass is shrunk (i.e, the pores are ejected), concentrated and increased in strength.

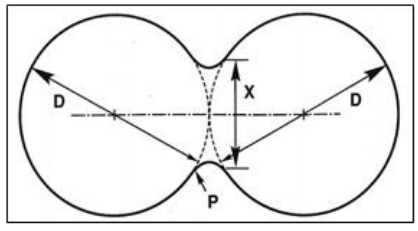

Figure 2. Sintering profile of two grains [18]

When two of the assemblies in Figure 3, are considered, there is a plurality of mating zones in the compressed powder pile. The bonds between the particles in contact with the progress of the sintering process expands and join. Each boundary grows one limit. As shown in Figure 3, the two particles are completely joined together as a result of a long sintering, resulting in a single sphere of 1.26 times the starting diameter.

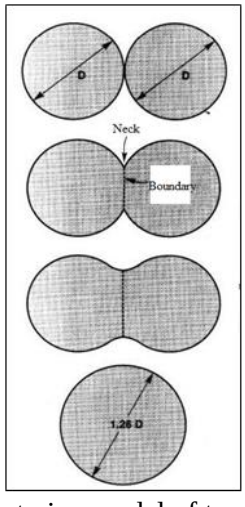

Figure 3. Sintering model of two grains [21]

تم استلام الورقة بتاريخ: 26 / 6 /2023م وتم نشرها على الموقع بتاريخ: 30 / 7 /2023م

As shown in Figure 4, a schematic diagram showing the change of the pore structure during sintering starting with the point contact of the particles is given. The space volume gradually decreases and gaps become more spherical. Clearly, it is clear that gaps are replaced by grain boundaries as globalization of space is formed.

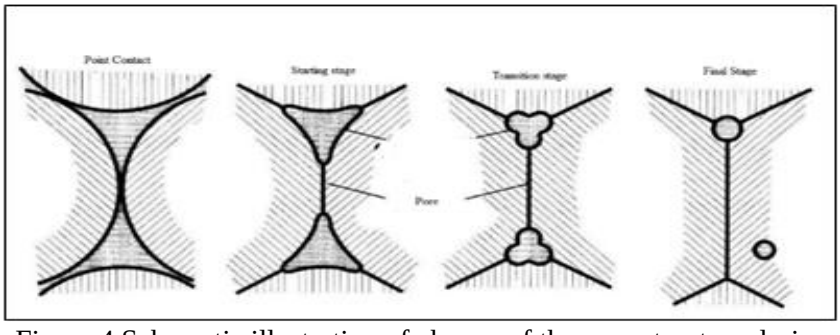

Figure 4.Schematic illustration of change of the pore structure during sintering [21]

2.1. Solid Phase Sintering

The solid phase sintering process is the result of intense condensation of the powder particles to the sintering temperature. The solid phase sintering process is shown in the diagram in Figure 5. In the diagram, solid-state sintering occurs in the X1 composition between A and B at temperature T1.

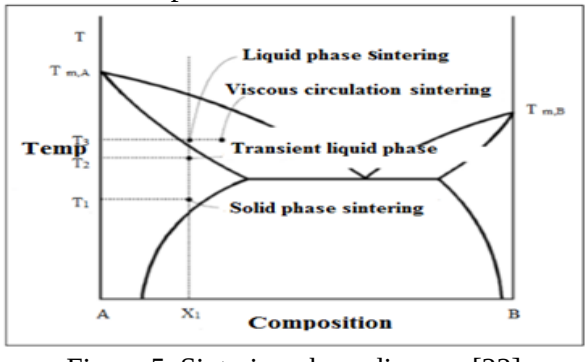

Figure 5. Sintering phase diagram [22]

تم استلام الورقة بتاريخ: 26 / 6 /2023م وتم نشرها على الموقع بتاريخ: 30 / 7 /2023م

2.2. Liquid Phase Sintering

The liquid phase sintering is sintered at the temperature at which the liquid phase is formed. A sudden shrinkage occurs by the formation of the liquid phase. During this shrinkage, the solid particles enter a new order in the liquid phase. Liquid phase sintering occurs when a liquid phase is formed in the powder during sintering. The diagram showing the liquid phase sintering is given in Figure 5. In the diagram, liquid phase sintering occurs in composition X1 at temperature T3. In liquid phase sintering, the amount of liquid phase cannot exceed 20 percent. In liquid phase sintering, ceramic powders can be sintered at low temperature and in short time. However, parts produced by liquid phase sintering are not suitable for use at high temperatures [21].

While the main powder remains solid during the sintering, the additive powder provides the liquid phase formation. Figure 6 consists of 4 parts. In the first part, the powders appear to be crude. In the second part, liquid phase propagation occurs. In the third section, the precipitation process occurs in the melt. Finally, in the fourth section, the liquid phase sintering process is finished and the solid skeleton of the material appears.

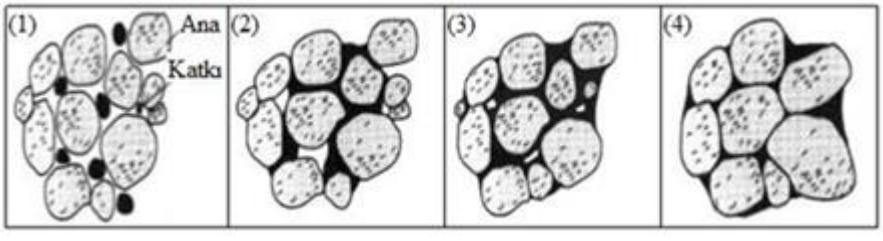

Figure 6. Stage of liquid phase sintering using two powder mixtures [22]

In Figure 7, grain growth occurs by re-precipitation of solids formed by the precipitation of small size grains on large grains. In addition to grain growth, the sintering process also gives the grain shape adjustment process. Thus, the solid is better packed and any remaining pore is thought to be better filled with liquid.

تم استلام الورقة بتاريخ: 26 / 6 /2023م وتم نشرها على الموقع بتاريخ: 30 / 7 /2023م

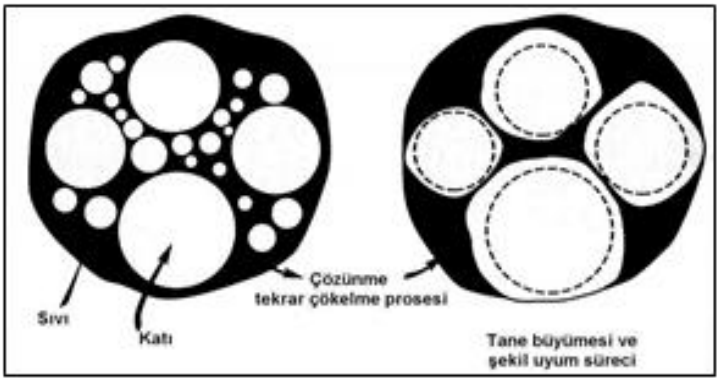

Figure 7. Precipitation and grain growth in liquid phase sintering process [22]

3. Experimental Work

In this study, firstly, gas atomization unit was used. In this gas atomization unit, production of AZ31 powder, which is magnesium alloy by gas atomization method from metal powder production methods, was chosen. The parameters used in the materials, which have similarity to AZ31 alloy as production parameters, are taken into consideration. Experimental studies were performed with three different parameters, temperatures, nozzle diameters,gas pressures were used,. In addition, in order to determine the usability of the powders produced, rectangle shaped of 32 mm length, 13 mm width and 7 mm thickness samples were manufactured. For this purpose, samples prepared at 600 MPa pressing pressure in one-way press were subjected to be sintered at different temperatures (500, 550 and 600 C°). Pre and post sintering densities of the prepared samples were determined and the pore amount and percentage of the samples were determined approximately.

Table 1. Chemical composition of AZ31 alloy

Material	Mg	AL	Zn	Mn
Content (%)	95.7144	2.77	1.1065	0.4015

تم استلام الورقة بتاريخ: 26 / 6 /2023م وتم نشرها على الموقع بتاريخ: 30 / 7 /2023م

Table 2. Chemical (XRF) analysis of produced AZ31 powders.

Material	Mg	AL	Zn	Mn	Si
Content (%)	94.71	2.75	1.62	0.61	0.22

Table 1 and Table 2 are examined as a powder with gas atomization. The chemical composition of the AZ31 material was found to be almost the same. Powder with gas atomization system shows how important it is in production.

3.1. Powders Pressing

The powders produced in different parameters and then mixed in the turbulent were subjected to pressing. The pressing process was carried out with HALIM USTA HIDROLIKSAN brand, illestrated in figure 8.

Figure 8. The pressing machine (HALIM USTA HIDROLIKSAN) branded

In the pressing process, a rectangular mold with a dimension of 30*13*7 mm was used as a die. Approximately 4.7 grams of powder was applied to each sample and pressed. Pressures of 600 MPa were

تم استلام الورقة بتاريخ: 26 / 6 /2023م وتم نشرها على الموقع بتاريخ: 30 / 7 /2023م

applied as the pressing pressure. Figure 9 shows the appearance of the raw material.

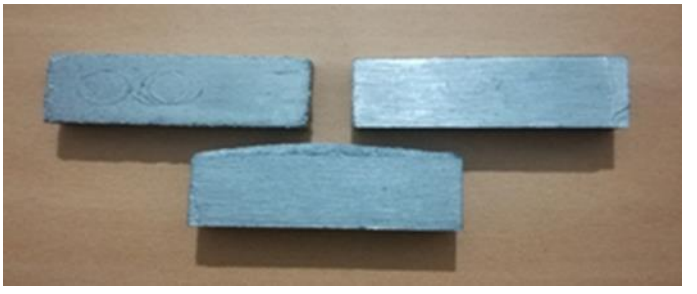

Figure 9. General view of pressed powder

3.2. Sintering of Powders

The samples , which were pressed and massed at pressure 600 MPa, were subjected to sintering in controlled furnace for two hours at three different temperatures (500, 550 and 600 C°).

In order to determine the optimum sintering temperatures, the parameters given in Table 3, were applied.

Table 3. Sintering parameters of samples

Sample No	Pressing Pressure MPa	Sintering Temperature C°
1	600	500
2		
3		550
4		
5		600
6		
7		

3.3.Sintering of Powdered Powders

The sintering process of the powders were carried out with an atmosphere controlled heat treatment furnace (PTF 16/80/610) as shown in (Figure 10).

تم استلام الورقة بتاريخ: 26 / 6 /2023م وتم نشرها على الموقع بتاريخ: 30 / 7 /2023م

Figure 10. Atmosphere controlled heat treatment furnace (PTF 16/80/610)

The sintering process was completed in a total of 180 minutes. In order to expel the wastes, they were raised to 500, 550 and 600 C°. Sintering temperatures were kept at a constant temperature for 120 minutes, the cooling zone in room temperature up to 180 minutes were cooled under atmospheric control.

3.4. Density Measurement

Sintered and post-sintered densities were measured to determine the optimum compressibility and sinterability of samples sintered at pressing 600 MPa and sintered at different temperatures (500, 550 and 600 C). Pre-sintering and post-sintering density values were measured separately for each sample. The determination of the densities was calculated by the ratio of the weight (m) / sample to the volume (v) of the sample produced. After these processes, the relative densities (% density) of the samples were determined. Calculated by the ratio of the weight (m) / sample to the volume (v) of the sample produced. After these processes, the relative densities (% density) of the samples were determined.Before sintering, density values of AZ31 alloys at 600 MPa were determined. Density values of massed samples are given in Table 4.

تم استلام الورقة بتاريخ: 26 / 6 /2023م وتم نشرها على الموقع بتاريخ: 30 / 7 /2023م

Table 4. Before sintering Density results of AZ31 alloys.

S. No	Pressing Pressure (MPa)	Weight (gr)	Length (cm)	Width (cm)	Thickness (cm)	Volume (cm^3)	Density (gr/cm^3	Relative Density (%)	Average Relative Density %
1	600	4.70	3.2	1.3	0.7	2.91	1.61	89.83	90.01
2		4.68	3.2	1.3	0.68	2.82	1.65	91.97	
3		4.69	3.2	1.3	0.71	2.95	1.58	88.23	
4		4.70	3.2	1.3	0.69	2.87	1.63	91.00	91.12
5		4.66	3.2	1.3	0.69	2.87	1.62	90.3668	
6		4.68	3.2	1.3	0.68	2.82	1.65	92.00	
7		4.68	3.2	1.3	0.685	2.84	1.64	91.29	91.123
8		4.71	3.2	1.3	0.70	2.91	1.61	89.85	
9		4.90	3.2	1.3	0.701	2.956	1.65	92.20	

Sample 7→ Weight = 4.683, Length =3.2, Width = 1.3, Thickness = 0.685.

Volume = Length * Width * Thickness = 3.2 * 1.3 * 0.685 = 2.8496 (cm3).

Density (ρ) = Weight/Volume = 4.683/2.8496 = 1.6433 (gr/cm3).

Relative Density (%) = Density (ρ)/1.8 = 1.6433/1.8 = 91.2993 (%).

After sintering density values of AZ31 alloys sintered at three different temperatures were determined. Sintering density values of massed samples are given in Table 5.

Table 5. Density results of sintered AZ31 alloys.

S.No	Pressing (MPa)	Sintering T. (C°)	Weight (gr)	L (cm)	W (cm)	T (cm)	V (cm^3)	Density (gr/cm^3)	Relative Density (%)	Average Relative Density (%)
1	600	500	4.48	3.17	1.28	0.66	2.67	1.67	93.06	93.78
2			4.66	3.18	1.29	0.67	2.75	1.69	94.16	
3			4.58	3.17	1.29	0.66	2.70	1.69	94.12	
4		550	4.19	3.15	1.26	0.64	2.54	1.65	91.81	85.80
5			3.3	3.15	1.27	0.63	2.52	1.34	74.72	
6			4.16	3.13	1.25	0.65	2.54	1.63	90.86	
7		600	4.37	3.18	1.27	0.64	2.58	1.69	93.99	92.24
8			3.81	3.15	1.27	0.58	2.32	1.64	91.22	
9			4.49	3.19	1.29	0.66	2.72	1.64	91.50	

تم استلام الورقة بتاريخ: 26 / 6 /2023م وتم نشرها على الموقع بتاريخ: 30 / 7 /2023م

When the density results given in Table 5 were examined, the average relative density of the samples sintered at 600 Cº was measured as 92.2418 %. However, the average relative density of the samples sintered at 500 Cº was measured as 93.7856 %. When Table 5 is examined, it is determined that the increasing density of the samples increases with decreasing sintering temperature.
The density values of AZ31 alloys, which were massed at constant pressures and then sintered at different temperatures, were determined. The density values were determined separately for each sample.

4. Image Analysis after Sintering Optical Microscope

Optical microscope images of AZ31 Mg alloy pressed powders, 600, 550 and 500 C° temperature and samples produced with pressures of 600 MPa. Figure 11.

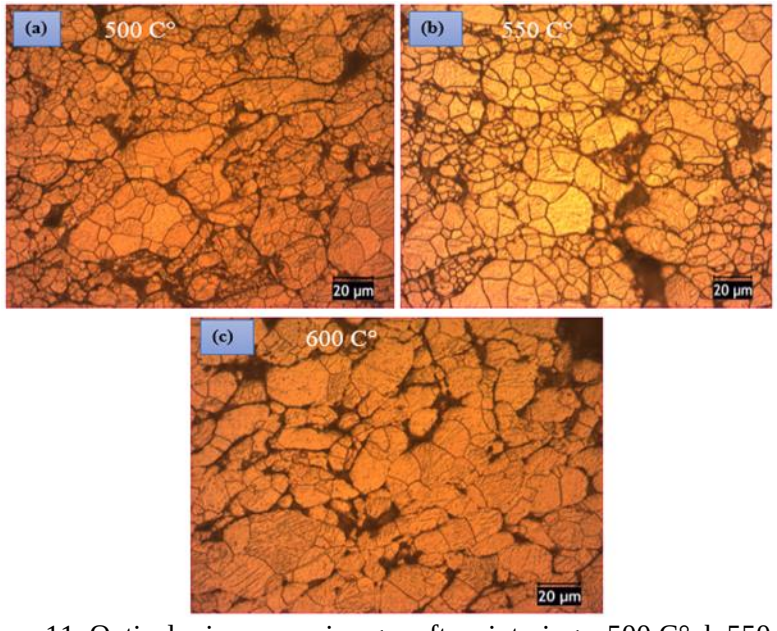

Figure 11. Optical microscope images after sintering a 500 C°, b 550 C°, c 600 C°, and 600 (MPa).

تم استلام الورقة بتاريخ: 26 / 6 /2023م وتم نشرها على الموقع بتاريخ: 30 / 7 /2023م

When the optical microscope images are examined, it is clear that the β (Mg17Al12) phase formed at the grain boundaries increases with the increase of temperature. In addition, the β (Mg17Al12) phase is clearly seen on the images given to surround the grains. In addition to this, it is observed that the β (Mg17Al12) phase with the effect of temperature not only spread on the grain boundaries but also throughout the structure [13,17].

5. SEM-EDS Analysis after Sintering

SEM images of samples produced with AZ31 Mg alloy at 600 MPa pressures and 500, 550 and 600 C° temperatures are shown in Figure 12. When the SEM images are examined, it is seen that the β (Mg17Al12) phase formed at the grain boundaries starts to spread to the surface with the increase of the temperature. In addition, the effect of temperature is clearly seen that the grains are shrinking. This can be explained by the increase in temperature and the increase of plastic deformation in powders. After a certain value, the powders are resistant to deformation and disintegration occurs.

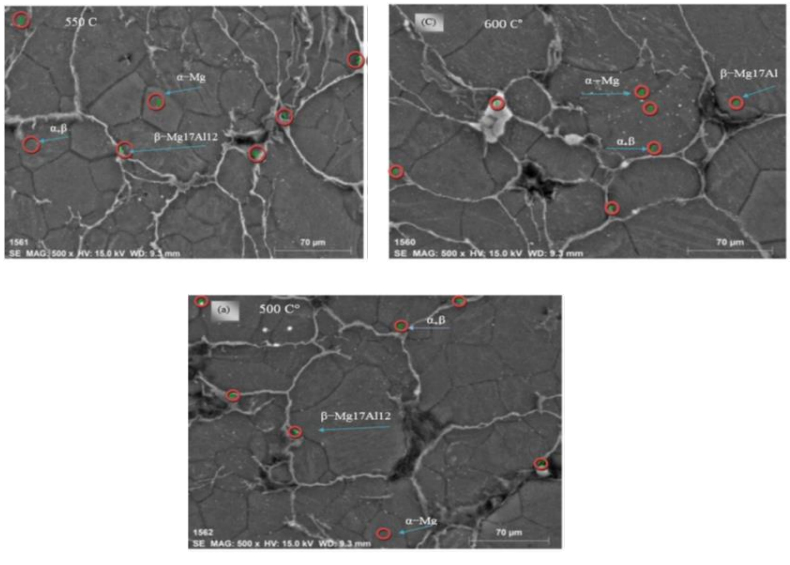

Figure 12. SEM images after sintering a 500 Co, b 550 Co, c 600 Co at 600 MPa

تم استلام الورقة بتاريخ: 26 / 6 /2023م وتم نشرها على الموقع بتاريخ: 30 / 7 /2023م

SEM images of the AZ31 Mg alloy with 600 MPa pressure and samples produced at 500, 550 and 600 C° are given in Figure 12. When the SEM images of the AZ31 alloy are examined, it is seen in Figure 12 that the other phases are distributed along the grain boundaries as well as the α-Mg matrix phase in the structure. Microstructure of the α-Mg matrix as well as grain boundaries with SEM-EDS analysis β (Mg17Al12) phase extending along and α + β eutectics as a fine phase at grain boundaries. Observed Figure 13.

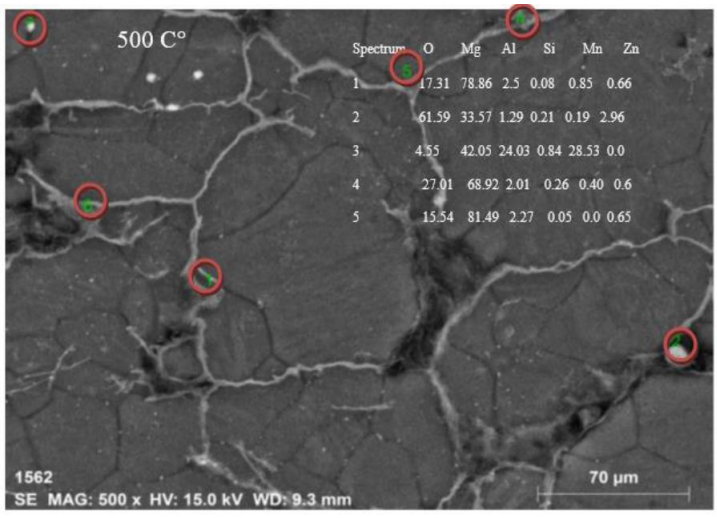

Figure 13. SEM-EDX image after sintering

High tendency of discrimination and the solid and liquid interface in the early stages of hardening during cooling. In a study conducted by Ünal et al [23], Al reported that enrichment with α-Mg forms an easy-fusion structure or phase β. Alpha-rich alpha-phase occurs in an area that does not reach enough composition to form an β-phase in the grain boundary**.**

تم استلام الورقة بتاريخ: 26 / 6 /2023م وتم نشرها على الموقع بتاريخ: 30 / 7 /2023م

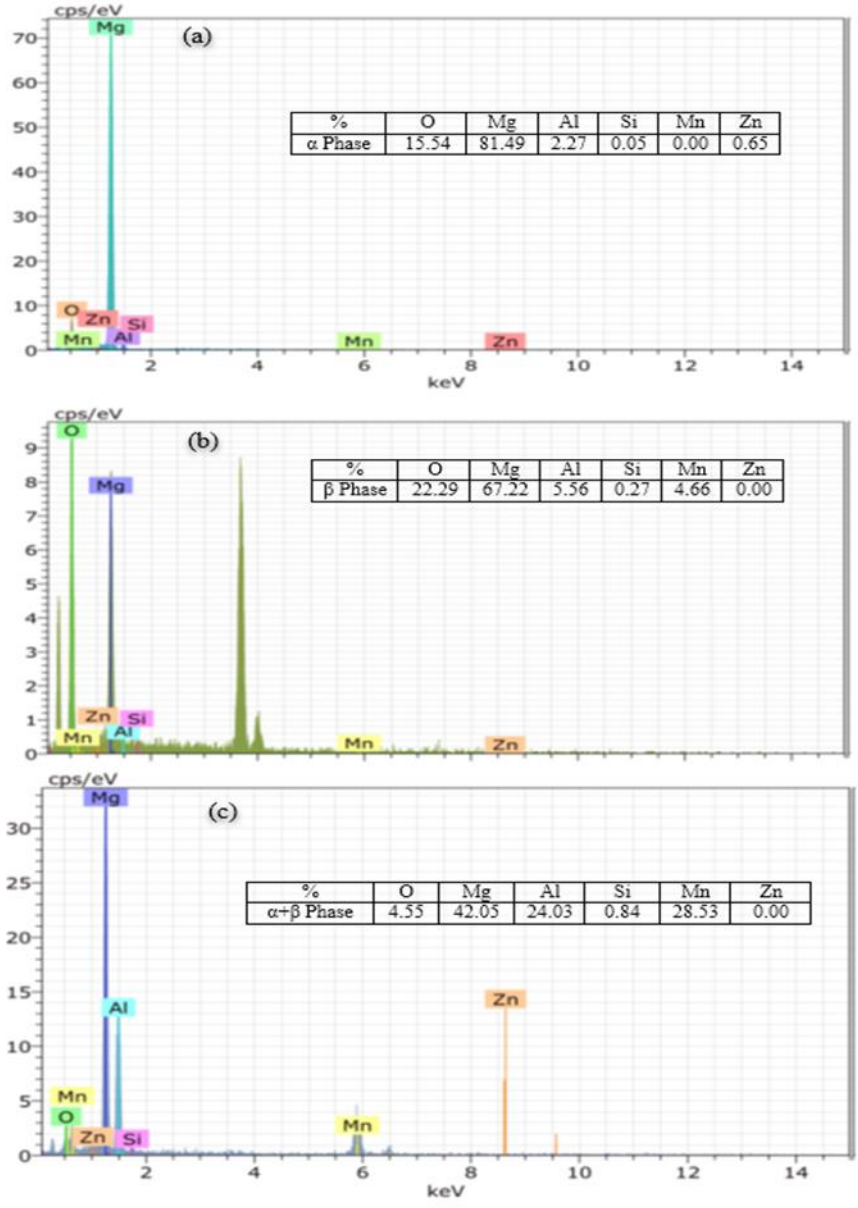

Figure 14. EDX analysis a) α phase EDX analysis, b) β phase EDX analysis, c) α + β phase EDX analysis.

تم استلام الورقة بتاريخ: 26 / 6 /2023م وتم نشرها على الموقع بتاريخ: 30 / 7 /2023م

6. General Results

1. At the end of XRF, the chemical composition of AZ31 powder and in got material were found to be close to the values.
2. As a result of XRD analysis, micro phase, phase α (Mg main matrix) phase β (Mg17Al12) was observed.
3. Sintered samples at three different temperatures (500, 550 and 600 C°) were determined and increase of their relative density after sintering was seen.
4. The sample having the highest relative density value after sintering process was measured at 600 MPa and at 500 C° it was 94,167%.

7. Discussion and Conclusion

After sintering, XRD measurements revealed that the structure con tained Mg, (Mg17Al12), and phases.XRD examination before sint ering, on the other hand, clearly indicated Mg peaks, whereas XR Danalysis after sintering revealed a modest decrease in the degree of Mg peaks.Furthermore, the phase of sintering XRD investigatio n revealed that the sintering temperature increasedand the Mg17Al 12 phase grew clearer.It was determined after sintering that the dec rease in Mg phase was caused by crystallization in thematerial. The cracks of the sintered materials were observed between the gra ins at high sintering temperatures, while the sintering temperature was reduced and the sintering surface was reflected in the SEM pic tures.Internal energies are thought to increase particle deformation and increase their size during flocculation.

REFERENCES

[1] Akra, K,., Boz, M.,The Production of Az31 Alloys by Gas Atomization Method and it's Characteristics, ", (Doktora tezi) *Karabuk University* (2019).

[2] Mordike, B.L., Ebert, T., "Magnesium Properties Applications Potential", *Mat. Sci. Eng. A*, 302: 37-45 (2001).

تم استلام الورقة بتاريخ: 26 / 6 /2023م وتم نشرها على الموقع بتاريخ: 30 / 7 /2023م

[3] Benedyk J.J., "Magnesium Challenges Aluminum Dominance as the Light Metal of Choice in Automotive Markets", *Light Metal Age-The International Magazine of Light Metal Industry*, (2004).

[4] American Society for Testing and Materials-ASM, Metal Handbook, Forming and Forging 9th Edition", 791-804 (1988).

[5] Kaya, A. A., Özdoğru, E.F., Abanoz, D., Yiğit, S., Yücel, O., "Otomotivde Magnezyum Alaşım Uygulamaları", OTEKON'02, *Otomotiv Teknolojileri Kongresi*, Bursa, (2002).

[6] Duygulu, Ö., Oktay, G., Kaya, A.A., "The Use of Magnesium Alloys in Automotive Industry", *OTEKON'06, Otomotiv Teknolojileri Kongresi*, Bursa, (2006).

[7] Kaya, A.A., Pekgüleryüz, M., Türkoğlu, S., Özdoğru, E.F., "Ağırlık Tasarrufu Amacıyla Otomobil Motor Bölmesinde Magnezyum Alaşımlarının Kullanımı", *OTEKON'04, Otomotiv Teknolojileri Kongresi*, Bursa, (2004).

[8] Fredrich, H., S. Schumann, "Research for a New Age of Magnesium in the Automotive Industry", *J. Mat. Proc. Tech.*, 117: 276-28, (2001).

[9] Furuya, H., Kogiso, N., Matunaga, S., Senda, K., "Applications of Magnesium Alloys for Aerospace Structure Systems", *Materials Science Forum*, 341-348, 350-351, (2001).

[10] Froes, F.H., Eliezer, D., Aghion, E., "The Science, Technology, and Applications of Magnesium", *J. Mat. Proc. Tech.*, 50 (9): 30-34, (1998).

[11] Chaffin, G.N., J.E., Jacoby, "Guidelines for Aluminum Sow Casting and Charging", *The Aluminum Association, Washington*, D.C., (1998).

تم استلام الورقة بتاريخ: 26 / 6 /2023م وتم نشرها على الموقع بتاريخ: 30 / 7 /2023م

[12] Gray, J.E., Luan, B., "Protective Coatings on Magnesium and its Alloys—A Critical Review", *J. Alloys Compd*., 336: 88-113, (2002).

[13] Kaya, R.A., Çavuşoğlu, H., Tanık, C., Kaya, A. A., Duygulu, Ö, Mutlu, Z., Zengin, E., Aydın Y., "The Effects of Magnesium Particles on Posterolateral Spinal Fusion: An Experimental in Vivo Study in a Sheep Model", *J.Neurosurg*-Spine, 6: 141-149, (2007).

[14] Duygulu, O., Kaya, R.A., Oktay, G. and Kaya, A.A., "Investigation on the Potential of Magnesium Alloy AZ31 as a Bone Implant", *Materials Science Forum*, 546-549: 421-424, (2007).

[15] Duygulu, O., Kaya, R.A., Oktay, G., Berk, C., and Kaya, A.A., "Can Magnesium Alloys be Used as Implants?- SEM Examinations from an in Vivo Study", *16th International Microscopy Conference*, Sopporo, Japan, (2006).

[16] Kaya, A.A., "Future of Magnesium: Applications in Transportation and Bone Surgery", *10th Int. Symposium on Advanced Materials (ISAM-2007)*, Islamabad, Pakistan, (2007).

[17] German, R. M. "Powder Metallurgy&Particule Metarials Procsessin" Çeviri Editörleri, *Süleyman SARITAŞ, Mehmet TÜRKER, Nuri DURLU, Türk Toz Metalurjisi Derneği*, 398-405 (2007).

[18] Göktaş, A.A., "AI2O3-B4C kompozit seramiklerin sinterlenmesi ve karakterizasyonu",.*Uluslar arası Metalurji ve Malzeme Kongresi*, İstanbul, 1317-1321 (1995).

تم استلام الورقة بتاريخ: 26 / 6 /2023م وتم نشرها على الموقع بتاريخ: 30 / 7 /2023م

[19] Ünlü, M. D., "SiC Esaslı Seramiklerin Spark Plazma Sinterleme(SPS) Yöntemi ile Üretimi ve Karakterizasyonu", (Doktora tezi) *Istanbul Technical University* (2014).

[20] Boz, M., "Toz Metalurjisi İle Üretilmiş Bronz Esaslı Fren Balata Malzemelerinin Sürtünme-Aşınma Davranışlarının İncelenmesi", Yüksek Lisans Tezi, *Gazi Üniversitesi Fen Bilimleri Enstitüsü,* Ankara (1999).

[21] German R.M., "Liquid Phase Sintering", *Plenum Press*, New York, 1-3 (1985).

[22] Avedesian, M.M., "Baker, H., Grades and alloys", in: ASM Speciality Handbook: *Magnesium and Magnesium Alloys, International ASM*, pp. 12e25 (1999).

[23] Ünal, R., "The influence of the pressure formation at the tip of the melt delivery tube on tin powder size and gas/melt ratio in gas atomization method", Journal of Materials Processing Technology, 180: 291–295 (2006).